J Herbmed Pharmacol. 2025; 14(3): 375-384.

http://www.herbmedpharmacol.com doi: 10.34172/jhp.2025.52787

Journal of Herbmed Pharmacology

Molecular docking and pharmacokinetic profiling of bioactive compounds from *Nigella sativa* L. and *Trigonella foenum-graecum* for targeting TNF-α and IL-6 in diabetic wounds

Maharani Retna Duhita*, Retno Susilowati, Siti Qurrotul Aini

Biology Study Program, Faculty of Science and Technology, Universitas Islam Negeri Maulana Malik Ibrahim, Malang, Indonesia

ARTICLE INFO

Article Type:
Original Article

Article History:
Received: 17 Oct. 2024
Revised: 27 Nov. 2024
Accepted: 4 Mar. 2025
Epublished: 1 Jul. 025

Keywords:
Anti-inflammatory agents
Diabetes mellitus
Herbal medicine
Molecular therapy
Signal transduction

ABSTRACT

Introduction: Diabetic wounds represent a significant challenge in the clinical management of people with diabetes. Current pharmacological approaches for diabetic wound treatment have demonstrated adverse effects, necessitating the investigation of alternative therapeutic agents, including extracts from *Nigella sativa* L. and *Trigonella foenum-graecum*. This study aimed to evaluate the therapeutic potential of bioactive compounds from a combination of those two extracts as new inhibitors of tumor necrosis factor-alpha (TNF-α) and interleukin-6 (IL-6), targeting their role in treating diabetic wounds.

Methods: This research employed in silico techniques, particularly pharmacokinetic analysis and molecular docking. The drug-like properties of bioactive compounds were analyzed using Swiss ADME. The ADMET predictions of bioactive compounds were analyzed using the pkCSM tool. Molecular docking analysis was performed using AutoDock Vina integrated in PyRx 0.8, and the binding between the active ingredients and 2AZ5 and 1P9M receptors was determined using BIOVIA Discovery Studio Visualizer.

Results: The results of ADME analysis explained that test compounds did not violate Lipinski's rule, were easily absorbed, and had good permeability. Furthermore, the results showed that all tested compounds had a safe LD50, but long-term use toxicity should be checked. Molecular docking results showed that *N. sativa* L. and *T. foenum-graecum* bioactive compounds inhibited TNF-α and IL-6.

Conclusion: All tested compounds may provide a safer alternative to synthetic treatments, but the most prominent compound for inhibiting TNF-α and IL-6 is yuccagenin. Further experimental studies are expected to validate its efficacy and safety in treating diabetic wounds.

Implication for health policy/practice/research/medical education:
This study has significant implications for research by highlighting the need to further validate the efficacy and safety of bioactive compounds from *Nigella sativa* and *Trigonella foenum-graecum* as potential treatments for diabetic wounds. This underscores the necessity for research into the underlying mechanisms of action to substantiate these findings. It also promotes interdisciplinary cooperation to investigate the creation of potent herbal compositions for treating diabetes.

Please cite this paper as: Duhita MR, Susilowati R, Aini SQ. Molecular docking and pharmacokinetic profiling of bioactive compounds from *Nigella sativa* L. and *Trigonella foenum-graecum* for targeting TNF-α and IL-6 in diabetic wounds. J Herbmed Pharmacol. 2025;14(3):375-384. doi: 10.34172/jhp.2025.52787.

Introduction

An unhealthy lifestyle can disrupt the body's balance, leading to various diseases, including diabetes mellitus (DM), a prevalent health issue globally (1). The International Diabetes Federation (IDF) anticipated a substantial rise in diabetes incidence by 2030, emphasizing the urgency of effective treatments. Complications of diabetes, such as diabetic wounds, can escalate to chronic conditions requiring amputation or resulting in death if not managed properly (2).

In theory, the interaction between tumor necrosis factor-alpha (TNF-α), interleukin-6 (IL-6), and other

***Corresponding author**: Maharani Retna Duhita,
Email: maharaniretna.duhita@uin-malang.ac.id

inflammatory mediators in diabetic wounds plays an important role in ongoing inflammation, impaired angiogenesis, oxidative stress, and cellular dysfunction. This mechanism can worsen tissue damage and slow wound healing, potentially causing chronic, non-healing wounds in diabetes patients (3). Although some drugs, such as bioplacenton offer healing potential, their side effects require the exploration of safer alternatives (4).

Nigella sativa L. and *T. foenum-graecum* are traditional medicines for treating diseases such as diabetic wounds. Ingredients found in *N. sativa*, such as thymoquinone, and in *T. foenum-graecum*, such as tigogenin, have shown anti-inflammatory, antibacterial, and antitumor activities. This is what makes these two plants used as natural medicines for skin diseases (5). *N. sativa* L. extract and *T. foenum-graecum* have shown promise in improving diabetic wound healing, yet their potential as TNF-α and IL-6 inhibitors remains underexplored (6). Recent studies indicate that these plant extracts enhance wound healing by increasing collagen density and fibroblast count while reducing inflammatory cell infiltration (2).

The discovery of new pharmaceuticals has predominantly depended on animal experimentation, which is both labor-intensive and costly. However, *in silico* methods, such as virtual screening, offer a promising alternative to overcome these limitations. By accelerating the discovery, identification, and analysis of active ingredients, in silico methods streamline the drug development process. Notably, molecular docking, an *in silico* technique, plays an essential function in forecasting the bioactivity of substances before laboratory analysis (7). Therefore, this study aimed to evaluate the therapeutic potential of bioactive compounds from *N. sativa* L. and *T. foenum-graecum* as new inhibitors of TNF-α and IL-6 for the treatment of diabetic wounds through *in silico* pharmacokinetic analysis and molecular docking methods.

Materials and Methods

Compound search and ligand structure preparation

The active compounds of *N. sativa* L. include thymoquinone, quercetin, beta amyrin, oleic acid, and linoleic acid; the active compounds of *T. foenum-graecum* include diosgenin, tigogenin, yuccagenin, smilagenin, and gitogenin (2). Neomycin acetate/neomix compound was used as a control. The compounds' structural data utilized in the ligand preparation were acquired from PubChem (https://pubchem.ncbi.nlm.nih.gov/) in a 3D format, specifically ".sdf.".

Protein target preparation

The RSCB PDB website provides resources for protein target preparation, including tumor TNF-α (PDB: 2AZ5) and IL-6 (PDB: 1P9M). Protein targets were extracted from water molecules (H2O) and their native ligands with Biovia Discovery Studio Visualizer v21.1.0.20298 (Figure 1) (7).

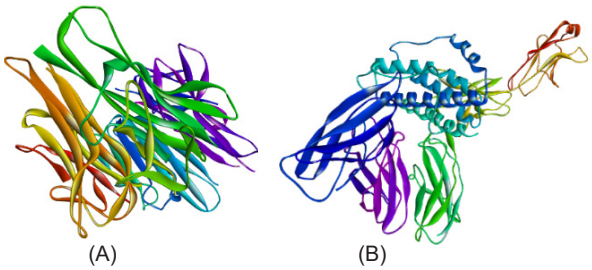

Figure 1. The structures of target proteins. A: TNF-α (2AZ5); B: IL-6 (1P9M). Their structures were examined to remove native ligands, heteroatoms, and water molecules using the software Biovia Discovery Studio Visualizer v21.1.0.20298.

Drug-likeness analysis

SwissADME (http://www.swissadme.ch/) was utilized to evaluate drug likeness based on *Lipinski's* law while examining the pharmacokinetics of the target compounds. SMILE obtained from PubChem was entered into SwissADME (Table 1) and compounds that met *Lipinski's* criteria were selected (8).

Absorption, distribution, metabolism, excretion, and toxicity (ADMET) prediction

Active compounds from extract combinations were identified for their ADMET profiles with the pkCSM online tool (https://biosig.lab.uq.edu.au/pkcsm/) (9).

Molecular docking method

Before docking the ligand to the target protein, the docking method was validated using PyRx. The test compound was then immobilized on the active site of the TNF-α receptor at the grid coordinates (x, y, z) or 71.6928 Å, 67.4813 Å, and 71.3257 Å. However, for the IL-6 receptor, the grid coordinates (x, y, z) were 123.0650 Å, 103.5787 Å, and 56.2382 Å. Molecular docking was performed using the PyRx AutoDock Vina 0.8 program in pdbqt file format. The validity of the molecular docking method parameters was evaluated using the root mean square deviation (RMSD) value. Validation of the molecular docking method was considered valid if the RMSD value was less than 2.0 Å. (10).

Visualization of docking results

The molecular docking simulation results were analyzed on the BIOVIA Discovery Studio application to determine ligands' 2D and 3D interactions with receptors by forming hydrogen bonds and binding patterns with other amino acid residues in the receptor's active site (11).

Results

Drug-likeness analysis

Drug-likeness was assessed using the SwissADME website and compared against the *Lipinski Rule of Five*, which focuses on the oral administration of pharmaceuticals. According to *Lipinski*, an effective pharmaceutical must

Table 1. Bioactive and simplified molecular input line entry system (SMILE) compound formula

Bioactive	Compound identification (CID)	SMILES
Thymoquinone	10281	CC1=CC(=O)C(=CC1=O)C(C)C
Quercetin	5280343	C1=CC(=C(C=C1C2=C(C(=O)C3=C(C=C(C=C3O2)O)O)O)O)O
Beta-amyrin	73145	CC1(CCC2(CCC3(C(=CCC4C3(CCC5C4(CCC(C5(C)C)O)C)C)C2C1)C)C)C
Oleic acid	445639	CCCCCCCC/C=C\CCCCCCCC(=O)O
Linoleic acid	5280450	CCCCC/C=C\C/C=C\CCCCCCCC(=O)O
Diosgenin	99474	CC1CCC2(C(C3C(O2)CC4C3(CCC5C4CC=C6C5(CCC(C6)O)C)C)C)OC1
Tigogenin	99516	CC1CCC2(C(C3C(O2)CC4C3(CCC5C4CCC6C5(CCC(C6)O)C)C)C)OC1
Yuccagenin	3083608	CC1CCC2(C(C3C(O2)CC4C3(CCC5C4CC=C6C5(CC(C(C6)O)O)C)C)C)OC1
Smilagenin	91439	CC1CCC2(C(C3C(O2)CC4C3(CCC5C4CCC6C5(CCC(C6)C)C)C)OC1
Gitogenin	441887	CC1CCC2(C(C3C(O2)CC4C3(CCC5C4CCC6C5(CC(C(C6)O)O)C)C)C)OC1

have a molecular weight (MW) of less than 500 g/mol, a log P of less than 5, fewer than ten hydrogen bond acceptors (HBA), and fewer than five hydrogen bond donors (HBD). The molar refractory (MR) criteria should be between 40 and 130. The *Lipinski Rule of Five* links physicochemical and pharmacokinetic features. Ligands that did not violate the two Lipinski rules were selected. The results showed that all tested compounds were candidates for further analysis (Table 2).

Prediction of physicochemical properties, pharmacokinetics, and toxicity (pkCSM)

The study used the pkCSM to predict pharmacokinetic and ADMET properties of drugs, focusing on absorption parameters such as human intestinal absorption, CaCo-2 cell permeability, and overall intestinal absorption. At the same time, distribution test parameters encompassed VDss, unbound fraction, and blood-brain barrier (BBB) (Table 3). The determinants for forecasting metabolism were CYP2D6 substrate, CYP3A4 substrate, CYP1A2 inhibitor, CYP2C19 inhibitor, CYP2C9 inhibitor, and CYP3A4 inhibitor (Table 4). Parameters for predicting excretion included overall clearance and renal OCT2 substrates. The parameters for toxicity investigation were AMES toxicity, oral rat acute toxicity lethal dosage (LD50), and hepatotoxicity (Table 5).

Molecular docking analysis and visualization

This work employed the PyRx tool for molecular docking to forecast the possible activity and interactions of drugs with protein targets (Table 6). All selected candidate compounds were predicted to have relatively low binding affinity (the more negative) with TNF-α. The list of compounds from the lowest binding affinity score in order included diosgenin (-10.2 kcal/mol), tigogenin and yuccagenin (-10.1 kcal/mol), beta-amyrin and gitogenin (-10 kcal/mol), smilagenin (-9.8 kcal/mol), quercetin (-8.8 kcal/mol), thymoquinone (-6.1 kcal/mol), oleic acid (-5.4 kcal/mol), linoleic acid (-5.2 kcal/mol) (Table 6). Most compounds, except oleic acid and linoleic acid, had lower binding affinity than neomycin sulfate as control (-6.4 kcal/mol). The lower affinity value indicates potential

Table 2. Evaluation of drug-likeness properties

Compound	Molecular weight (MW)	LogP	Hydrogen bond acceptors (HBA)	Hydrogen bond donors (HBD)	Molecular refractivity (MR)	Violation
Thymoquinone	164.20 g/mol	1.85	2	0	47.52	0
Quercetin	302.24 g/mol	1,23	7	5	78.03	0
Beta-amyrin	426.72 g/mol	7.18	1	1	134.88	2
Oleic Acid	282.46 g/mol	5.71	2	1	89.94	1
Linoleic Acid	280.45 g/mol	5.45	2	1	89.46	1
Diosgenin	414.62 g/mol	5.01	3	1	121.59	1
Tigogenin	416.64 g/mol	5.22	3	1	122.07	1
Yuccagenin	430.62 g/mol	4.14	4	2	122.76	0
Smilagenin	416.64 g/mol	5.22	3	1	122.07	1
Gitogenin	432.64 g/mol	4.43	4	2	123.23	0

Notes: Molecular weight (MW) should be less than 500 g/mol; LogP should be between -0.4 and 5; Hydrogen bond acceptors (HBA) should be less than 10; Hydrogen bond donors (HBD) should be less than 5; Molecular refractivity (MR) should be between 40 and 130; Violations indicate the number of criteria violated according to *Lipinski's rule*.

Table 3. Results of absorption and distribution profile analysis of potential inhibitors

Compound	Absorption			Distribution	
	Water solubility (Log S)	CaCO2 permeability (log cm/s)	Intestinal absorption (%)	VDss (L/kg)	BBB permeability (log BB)
Thymoquinone	-1.613	1.271	99.382	-0.026	0.326
Quercetin	-2.925	-0.229	77.207	1.559	-1.098
Beta-amyrin	-6.531	1.226	93.733	0.268	0.667
Oleic Acid	-5.924	1.563	91.823	-0.558	-0.168
Linoleic Acid	-5.862	1.57	92.329	-0.587	-0.142
Diosgenin	-5.539	1.293	96.565	0.426	0.2
Tigogenin	-5.485	1.301	95.856	0.174	0.17
Yuccagenin	-5.096	1.264	96.811	0.005	0.119
Smilagenin	-5.485	-5.485	95.856	0.174	0.17
Gitogenin	-5.01	1.272	96.101	-0.259	0.089

Table 4. Results of metabolic profile analysis of potential inhibitors

Compound	CYP Substrate		CYP Inhibitor				
	2D6	3A4	1A2	2C19	2C9	2D6	3A4
Thymoquinone	No	No	No	No	No	No	No
Quercetin	No	No	Yes	No	No	No	No
Beta-amyrin	No	Yes	No	No	No	No	No
Oleic Acid	No	Yes	Yes	No	No	No	No
Linoleic Acid	No	Yes	Yes	No	No	No	No
Diosgenin	No	Yes	No	No	No	No	No
Tigogenin	No	Yes	No	No	No	No	No
Yuccagenin	No	Yes	No	No	No	No	No
Smilagenin	No	Yes	No	No	No	No	No
Gitogenin	No	Yes	No	No	No	No	No

Table 5. Results of excretion profile and toxicity analysis of potential inhibitors

Compound	Excretion		Toxicity		
	Total clearance (mL/min)	Renal OCT2 substrate	AMES toxicity	Oral rat acute toxicity (LD50)	Hepatotoxicity
Thymoquinone	0.225	No	No	1.743	Yes
Quercetin	0.407	No	No	2.471	No
Beta-amyrin	-0.044	No	No	2.478	No
Oleic Acid	1.884	No	No	1.417	No
Linoleic Acid	1.936	No	No	1.429	Yes
Diosgenin	0.328	Yes	No	1.921	No
Tigogenin	0.322	No	No	2.052	No
Yuccagenin	0.348	Yes	No	2.062	No
Smilagenin	0.322	No	No	2.052	No
Gitogenin	0.342	No	No	2.175	No

candidates as TNF-α inhibitors, as the active compound binds more easily to TNF-α.

The results of the interaction between compounds and IL-6 from the lowest binding affinity scores in the order included beta-amyrin (-10.2 kcal/mol), diosgenin (-9.7 kcal/mol), gitogenin (-9, 6 kcal/mol), yuccagenin (-9.3 kcal/mol), tigogenin (-8.9 kcal/mol), smilagenin (-8.4 kcal/mol), quercetin (-7.9 kcal/mol), thymoquinone (-5.2 kcal/mol), linoleic acid (-4.6 kcal/mol), oleic acid (-4.3 kcal/mol) (Table 6). Most compounds, except thymoquinone,

Table 6. Binding affinity and chemical interaction between test compound and target protein

Protein	Compound	Binding affinity (kcal/mol)	Interaction point	Bond type
2AZ5 TNF-α	Neomycin sulfate	-6,4	LEU57, ILE155, HIS15, LEU57, GLN61, TYR119, LEU120, GLY121	Van der Waals
			TYR59	Pi-sigma
			SER60, TYR151, GLN149	Conventional hydrogen bond
	Thymoquinone	-6,1	TYR59, SER60, GLN61, LEU120, GLY121, TYR151	Van der Waals
			TYR119	Pi-sigma
	Quercetin	-8,8	-	-
	Beta amyrin	-10	TYR59, SER60, TYR119, LEU120	Van der Waals
			GLY121, TYR151	Conventional hydrogen bond
	Oleic acid	-5,4	TYR59, TYR119, TYR151	Pi-alkyl
			SER60	Conventional hydrogen bond
			GLN61, LEU120, GLY121	Van der Waals
	Linoleic acid	-5,2	LEU120, SER60, GLN61, GLN61, TYR119, ILE155	Van der Waals
			TYR59	Pi-sigma
			TYR151	Conventional hydrogen bond
			LEU57	Alkyl
	Diosgenin	-10,2	LEU120, SER60, GLN61, GLY121, TYR151, LEU57, ILE155, HIS15	Van der Waals
			TYR59	Carbon hydrogen bond
	Tigogenin	-10,1	LEU120, SER60, GLN61, GLY121, -TYR151, ILE155	Van der Waals
			TYR59, TYR119	Pi-alkyl
			LEU57	Alkyl
	Yuccagenin	-10,1	TYR59, TYR119	Pi-alkyl
			SER60, TYR151, GLY121, ILE155, HIS15, LEU57	Van der Waals
	Smilagenin	-9,8	LEU120, SER60, GLN61, GLY121, TYR151, LEU57, ILE155, HIS15	Van der Waals
			TYR59	Pi-alkyl
	Gitogenin	-10	TYR59	Carbon hydrogen bond
			SER60, GLN62, GLY121, TYR151, LEU57, ILE155, HIS15, ARG1045	Van der Waals
			TYR119	Pi-alkyl
1P9M IL-6	Neomycin sulfate	-7,0	SER166, LYS66, ASN61, SER169, SER137, PHE134, ASN136	Conventional hydrogen bond
			ARG168, GLN135	Carbon hydrogen bond
	Thymoquinone	-5,2	-	-
	Quercetin	-7,9	-	-
	Beta amyrin	-10,2	SER166	Conventional hydrogen bond
			PHE134	Pi-alkyl
	Oleic Acid	-4,3	PHE134	Conventional hydrogen bond
	Linoleic Acid	-4,6	-	-
	Diosgenin	-9,7	PHE134	Pi-alkyl
	Tigogenin	-8,9	-	-
	Yuccagenin	-9,3	PHE134	Pi-sigma
			ARG168, SER166, LYS66, ASN136, GLN135	Van der Waals
	Smilagenin	-8,4	-	-
	Gitogenin	-9,6	-	-

TNF-α, tumor necrosis factor-alpha; IL-6, interleukin-6.

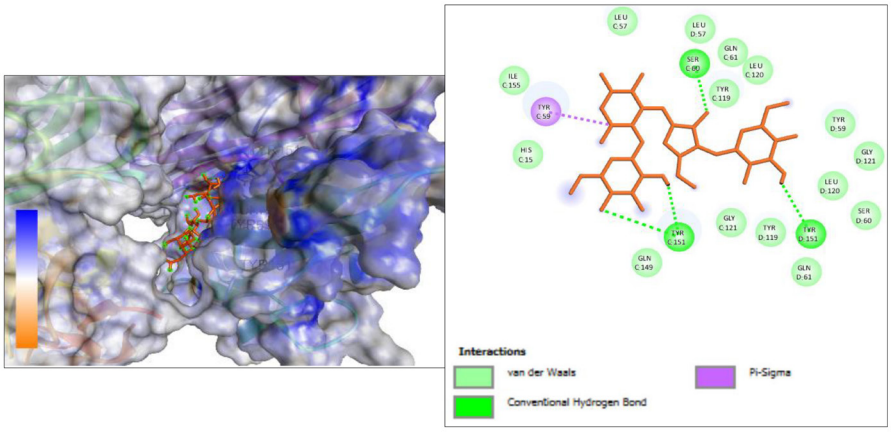

Figure 2. Binding conformation of neomycin sulfate in the active site of TNF-α receptor (2AZ5) 3D (Left) and 2D (Right).

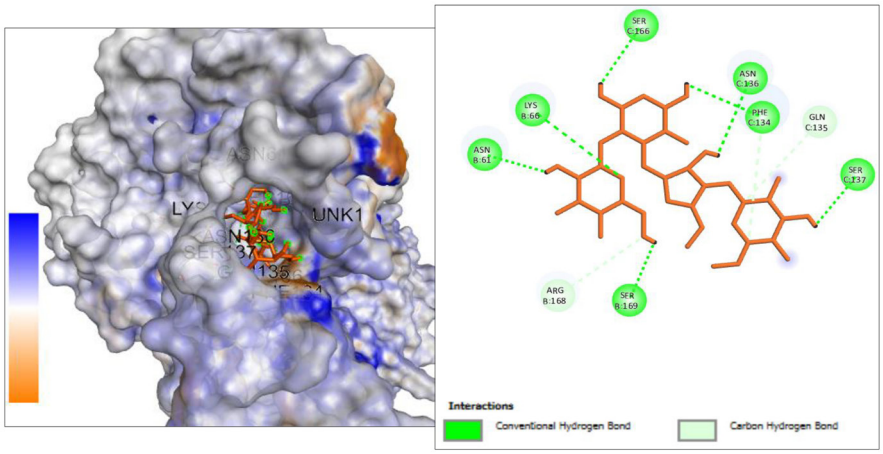

Figure 3. Binding conformation of neomycin sulfate in the active site of IL-6 receptor (1P9M) 3D (Left), and 2D (1P9M) (Right).

oleic acid, and linoleic acid had lower binding affinity than neomycin sulfate as control (-7.0 kcal/mol), indicating potential candidates as IL-6 inhibitors.

The visualization outcomes of chemical interactions between the test chemicals and the target proteins are presented in Table 6. These macromolecules were selected to assess the ability of the test compounds to interact with TNF-α and IL-6, which are inflammatory receptors. Analysis of the interaction characteristics between neomycin sulfate and TNF-α macromolecules showed that this ligand could bind to the active site through van der Waals bonds formed at amino acid residues (LEU57, ILE155, HIS15, LEU57, GLN61, TYR119, LEU120, and GLY121). In comparison, pi-sigma bonds were formed on amino acid residue (TYR59). Conventional hydrogen bonds were formed on amino acid residues (SER60, TYR151, and GLN149). Based on their interactions with the TNF-α binding site, beta-amyrin, an active compound from *N. sativa* L., and diosgenin, an active compound from *T. foenum-graecum*, demonstrated the most similar interactions with the neomycin sulfate ligand compared to other compounds.

Visualization of molecular docking of neomycin sulfate compound as a control with IL-6 receptor showed that this ligand could bind to the active side of IL-6 through conventional hydrogen bond formed at amino acid residues (SER166, LYS66, ASN61, SER169, SER137, PHE134, and ASN136). Carbon hydrogen bonds were formed on amino acid residues (ARG168, GLN135). Based on its interaction with the IL-6 binding site, beta-amyrin, which is an active compound from *N. sativa* L., and diosgenin, an active compound from *T. foenum-graecum*, showed the most similar interaction with neomycin sulfate ligand compared to other compounds.

Visualization of the interaction between neomycin sulfate which acts as a control in the interaction with TNF-α and IL-6 macromolecules (Figures 2 and 3). The binding mode of neomycin sulfate in the TNF-α macromolecular complex was examined from its crystal structure (PDB ID: 2AZ5). Neomycin sulfate binds to the active site of TNF-α (Figure 2) through Van der Waals bonds with LEU57, ILE155, HIS15, LEU57, GLN61, TYR119, LEU120, and GLY121. In addition, it can bind to the active site of TNF-α through pi-sigma bonds with TYR59, and conventional hydrogen bonds with SER60, TYR151, and GLN149.

The binding mode of neomycin sulfate in the IL-6 macromolecular complex was examined from its crystal structure (PDB ID: 1P9M). Analysis of the interaction characteristics between neomycin sulfate and macromolecules (Figure 3) shows that neomycin sulfate can bind to the active site of IL-6 through conventional hydrogen bonds with SER166, LYS66, ASN61, SER169, SER137, PHE134, and ASN136. In addition, it can bind to the active site of IL-6 through hydrogen bonds with ARG168, and GLN135. These interactions indicate that neomycin sulfate can bind specifically to both macromolecules, which has the potential to affect its biological activity. The most potential drug candidates when ranked based on a combination of affinity, Lipinski's rule, GI absorption, and toxicity tests are as follows: Diosgenin > gitogenin > yuccagenin > tigogenin > smilagenin > thymoquinone > linoleic acid > oleic acid > quercetin > beta-amyrin (Tabel 7).

Discussion

This study evaluated the potential of *N. sativa* L. and *T. foenum-graecum* as therapeutic agents for diabetic wounds using an in-silico approach. Previous experimental studies suggested combining those two extracts could be used as treatment agents for diabetic incision wounds in streptozotocin-induced mice. However, the specific bioactive compounds responsible for their anti-inflammatory and antibacterial effects remain unidentified (2).

This study employed SwissADME, a web-based application, to evaluate the potential of compounds from *N. sativa* L. and *T. foenum-graecum* as established synthetic drugs for diabetic wound treatment, focusing on physicochemical properties, pharmacokinetics, drug similarity, and drug safety, with efficient data processing and interpretation (12,13). According to the outcomes of the *Lipinski Rule of Five* evaluation, all tested compounds meet the rules (Table 2) so that they can be given orally (7). Compounds with MW <500 g/mol can be absorbed well and have high permeability in the intestinal tract. Conversely, compounds with MW >500 g/mol take a long time to absorb and have low intestinal tract permeability (13).

The log *P* value of a compound impacts its ability to penetrate the plasma membrane, distribution process, and affinity to plasma proteins. The optimal log P value is ≤5, as larger values can lead to higher toxicity due to longer retention in the lipid bilayer and reduced binding selectivity to target enzymes. Negative log *P* values are unfavorable as they cannot traverse the lipid bilayer membrane. The *Lipinski Rule of Five* delineates the solubility of specific substances in cell membranes via passive diffusion, emphasizing optimal values for HBD and HBA (13).

Absorption profiles were assessed, encompassing water solubility, CaCO2 permeability, intestinal absorption, and dermal permeability. Water solubility denotes a molecule's solubility in water at 25 °C, while lipophilic medicines exhibit reduced absorption. Beta-amyrin has a water solubility value above 6. CaCO2 cells predict drug absorption in the human intestinal mucosa, providing a barrier for ions and small molecules. High CaCO2 permeability values reflect high permeability, whereas low CaCO2 permeability values signify limited permeability (14). HIA refers to the absorption of drugs in the intestine from orally administered solutions. Intestinal absorption is said to be good if it has a percentage value of >80% and poor if the percentage is <30% (15). All compounds except quercetin compounds showed good absorption values of >80%.

The distribution test parameters included VDss (volume of distribution at steady state), fraction unbound, and BBB penetration (Table 3). The VDss is a theoretical value representing the volume in which a drug would need to be uniformly distributed to match the concentration in the plasma. A higher VDss indicates that more of the drug is distributed in tissues rather than plasma, suggesting better tissue solubility and a larger distribution volume. Conversely, a lower VDss means more drugs remain in the plasma. Drug distribution is also influenced by its binding

Table 7. Summary of *Lipinski*, ADME, toxicity, and molecular docking test results as a diabetic wound drug candidate

Active compound	Lipinski	Absorption	Distribution	Metabolism	Excretion	Toxicity class	Binding affinity (kcal/mol) TNF-α	Binding affinity (kcal/mol) IL-6
Thymoquinone	Yes	High	High	Yes	Yes	4	-6.1	-5.2
Quercetin	Yes	Medium	Low	Yes	Yes	5	-8.8	-7.9
Beta-amyrin	No	High	High	Yes	Yes	5	-10	-10.2
Oleic Acid	Yes	High	High	Yes	Yes	4	-5.4	-4.3
Linoleic Acid	Yes	High	High	Yes	Yes	4	-5.2	-4.6
Diosgenin	Yes	High	High	Yes	Yes	4	-10.2	-9.7
Tigogenin	Yes	High	High	Yes	Yes	5	-10.1	-8.9
Yuccagenin	Yes	High	High	Yes	Yes	5	-10.1	-9.3
Smilagenin	Yes	High	High	Yes	Yes	5	-9.8	-8.4
Gitogenin	Yes	High	High	Yes	Yes	5	-10	-9.6

TNF-α, tumor necrosis factor-alpha; IL-6, interleukin-6.

to serum proteins. Drugs in plasma exist in equilibrium between their unbound forms and protein-bound forms. The higher the protein binding, the less efficient the drug's ability to permeate cell membranes through diffusion (15). VDss is considered low if it is below <-0.15 and high if it is >0.45. VDss compounds with low values were oleic acid, linoleic acid, and gitogenin compounds.

The BBB safeguards the human brain from external chemicals. The capacity of medications to traverse the BBB is a critical factor that must be evaluated to alleviate side effects and toxicity while augmenting the efficacy of pharmaceuticals that exert their pharmacological effects on the brain. In animal models, blood-to-brain permeability is quantified in vivo as logBB, the logarithmic ratio of drug concentration in brain plasma (15). A compound with a logBB >0.3 can readily traverse the BBB. In contrast, a molecule with a logBB <0.3 is regarded as having difficulty crossing the BBB. The pkCSM prediction results indicate that the molecule quercetin has a distribution value of -1.098 (Table 3), which suggests a poor permeability to the BBB, as it exceeds -1.

Cytochrome P450 is a crucial enzyme in the body, predominantly in the liver. Cytochrome P450 oxidizes xenobiotics to inactivate pharmaceutical drugs. It is essential to evaluate the capacity of drugs to inhibit cytochrome P450. Cytochrome comprises multiple isoform models, specifically CYP1A2, CYP2C19, CYP2C9, CYP2D6, and CYP3A4. Pharmaceuticals can inhibit or stimulate cytochrome P450 enzymes, resulting in significant drug-drug interactions that may cause unexpected side effects, reactions, or treatment failures. Therefore, caution should be used when prescribing drugs that are known inhibitors or inducers of CYP450. Depending on the potential for decreased or increased metabolism, the targeted agent may need to be changed or the dosage adjusted (16). The parameters for the excretion test included total clearance (CLtotal) and organic cation transporter 2 (OCT2). Drug clearance (CL total) remains relatively constant and results from the combined contributions of hepatic clearance, which includes liver metabolism and biliary excretion, and renal clearance, which is responsible for elimination via the kidneys. A compound excretion is good if the MW is small and hydrophilic. If the high MW has hydrophobic properties, the smaller compound can potentially cause toxicity (15). As shown in Table 5, linoleic acid exhibits the highest total clearance, indicating it is rapidly excreted from the body. In contrast, beta-amyrin demonstrates low clearance values, suggesting a potential for accumulation and toxicity in the body.

OCT2 is a renal transporter that facilitates kidney drug and endogenous compound clearance. It can affect OCT2 substrates, potentially leading to adverse interactions with OCT2 inhibitors (15). The pkCSM prediction (Table 5) indicates that diosgenin and yuccagenin compounds can affect OCT2 substrates. Toxicities of compounds can be determined using the Ames Toxicity test, oral rat acute toxicity, Lethal dose (LD50), and hepatotoxicity. Positive results indicate mutagenic potential and potential carcinogenicity (17). However, none of the tested compounds exhibited mutagenic or carcinogenic effects. AMES toxicity, oral rat acute toxicity (LD50), and hepatotoxicity measurements play an important role in evaluating the safety profile of bioactive compounds in the drug discovery or development process. These evaluations provide valuable insight into the potential hazards associated with a compound and provide a more comprehensive understanding of its safety profile. The clinical relevance of these evaluations lies in their ability to guide decision-making and mitigate risks while developing new, safer, and more effective therapeutic agents (18).

Table 5 shows that thymoquinone (1743 mg/kg), oleic acid (1417 mg/kg), linoleic acid (1429 mg/kg), and diosgenin (1921 mg/kg) have LD50 values placing them in class 4 (300 < LD50 ≤ 2000 mg/kg), indicating relatively low toxicity. In contrast, quercetin (2471 mg/kg), beta-amyrin (2478 mg/kg), tigogenin (2052 mg/kg), yuccagenin (2062 mg/kg), smilagenin (2052 mg/kg), and gitogenin (2175 mg/kg) fall under class 5 (2000 < LD50 ≤5000 mg/kg), indicating low toxicity (19). In the hepatotoxicity test, two compounds were potentially toxic to the liver: thymoquinone and linoleic acid. Hepatotoxicity is a condition in which liver cells are damaged by toxic chemical compounds (20).

Target proteins were TNF-α and IL-6 because diabetes is characterized by chronic inflammation, as evidenced by increased expression of pro-inflammatory cytokines such as TNF-α and IL-6; this will cause increased inflammation and chronicity in wounds. Inhibition of TNF-α and IL-6 is essential for wound care by reducing inflammation, which shows its usefulness in its application to diabetic wounds (6,21).

Molecular docking is used to determine the interaction of ligands with macromolecules because of its ability to predict with a high degree of accuracy and ligand conformation in the right target binding site. Target proteins used were TNF-α (PDB: 2AZ5) with a resolution of 2.10 Å and IL-6 (PDB: 1P9M) with a resolution of 3.65 Å in human organisms with a measurement method using X-ray diffraction, although with a rather low resolution but sufficient for in silico testing (22,23).

The study found that the bioactive compounds *N. sativa* L. and *T. foenum-graecum* were inhibitors of TNF-α and IL-6. The parameters analyzed in the molecular docking process were the RMSD value, free binding energy (ΔG), hydrogen bonds, and other interaction patterns with amino acid residues on the active side of the receptor. An RMSD value of less than 2 Å indicates that the molecular docking method parameters provide results closer to the experimental results (10). From the validation results, an RMSD value of 0.0 Å was obtained, which means that the parameters of the molecular docking method used met

the requirements. A smaller RMSD indicates a more stable bond between the ligand and the protein (24).

The free binding energy value measures the ability of a drug to bind to a receptor, with negative values indicating good ligand-receptor bond stability. A more negative free binding energy value indicates a higher stability level between the ligand and the target protein (receptor), resulting in a stronger bond formation. The docking results in Table 6 show that the lowest free binding energy value is when the beta amyrin compound interacts with all target proteins. The binding free energy value is -10.0 kcal/mol when interacting with TNF-α and -10.2 kcal/mol when interacting with IL-6. This compound is the most stable and optimal drug candidate among *N. sativa* L. derivatives. Molecular docking results showed that the diosgenin compound had the lowest binding free energy value when interacting with all target proteins. The binding free energy value is -10.2 kcal/mol when interacting with TNF-α and -9.7 kcal/mol when interacting with IL-6. The affinity of the diosgenin compound makes it the most stable and optimal drug candidate among *T. foenum-graecum* compounds. The results of the molecular docking simulation were visualized using Discover Studio Visualizer v21.1.0.20298. Observing the interaction between amino acid residues aims to identify the interactions between ligands and receptors. Hydrogen bonds are interactions that can stabilize ligand binding to receptors. Other interactions between ligands that can increase conformational stability include electrostatic interactions and van der Walls interactions.

Neomycin sulfate forms various bonds with TNF-α and IL-6, including pi-sigma, van der Waals, and hydrogen bonds, as shown in Figure 2. Analysis of the interaction characteristics between neomycin sulfate can bind to the active site of TNF-α through conventional hydrogen bonds with SER60, TYR151, GLN149, and Van der Waals bonds with LEU57, ILE155, HIS15, LEU57, GLN61, TYR119, LEU120, GLY121, and pi-sigma bonds with TYR59. Based on their interactions with the active site of TNF-α, beta amyrin, and diosgenin showed the most similar interactions with neomycin sulfate ligands compared to other compounds. Meanwhile, the analysis of the interaction characteristics between neomycin sulfate can bind to the active site of IL-6 through conventional hydrogen bonds with SER166, LYS66, ASN61, SER169, SER137, PHE134, ASN136, and hydrogen bonds with ARG168, GLN135. Based on their interactions with the active site of IL-6, beta amyrin, and diosgenin showed the most similar interactions with the neomycin sulfate ligand compared to other compounds.

Conclusions

Beta-amyrin and diosgenin had similar interaction properties to neomycin sulfate. However, yuccagenin is the most recommended compound for inhibiting TNF-α and IL-6. The primary compounds of *N. sativa* L. and *T. foenum-graecum* represent an optimal combination for treating diabetic wounds. Therefore, conducting clinical trials to evaluate the safety and effectiveness of this combined extract will provide valuable insights into its therapeutic potential. While AutoDock Vina is a widely used and reliable molecular docking tool, it does have limitations. For future studies, it is recommended to incorporate the updated version of AutoDock Vina. This update will refine the docking process and potentially provide more precise predictions of molecular interactions, thereby further improving the therapeutic evaluation of the compounds.

Acknowledgments

Thanks to the Faculty of Science and Technology at Universitas Islam Negeri Maulana Malik Ibrahim for allowing us to guide bioinformatics lessons.

Authors' contribution

Conceptualization: Maharani Retna Duhita, Siti Qurrotul Aini.
Data curation: Maharani Retna Duhita, Siti Qurrotul Aini.
Formal analysis: Maharani Retna Duhita, Siti Qurrotul Aini.
Funding acquisition: Maharani Retna Duhita, Retno Susilowati,
Investigation: Maharani Retna Duhita, Siti Qurrotul Aini.
Methodology: Maharani Retna Duhita, Siti Qurrotul Aini.
Project administration: Maharani Retna Duhita, Retno Susilowati
Resources: Maharani Retna Duhita, Retno Susilowati, Siti Qurrotul Aini.
Supervision: Maharani Retna Duhita, Siti Qurrotul Aini.
Validation: Maharani Retna Duhita, Siti Qurrotul Aini.
Visualization: Maharani Retna Duhita, Siti Qurrotul Aini.
Writing–original draft: Maharani Retna Duhita, Siti Qurrotul Aini.
Writing-review & editing: Maharani Retna Duhita, Siti Qurrotul Aini.

Conflict of interests

The authors declare that they hold no competing interests.

Ethical considerations

The study protocol was approved by the Ethics Committee for Health Research, Faculty of Science and Technology, Universitas Islam Negeri Maulana Malik Ibrahim Malang, Indonesia (approval reference number: 020/EC/ KEP-FST/2020).

Funding/Support

This work was supported by Universitas Islam

Negeri Maulana Malik Ibrahim Malang International Collaborative Development Research, grant number 1224, Year 2023.

References

1. Yan Y, Wu T, Zhang M, Li C, Liu Q, Li F. Prevalence, awareness and control of type 2 diabetes mellitus and risk factors in Chinese elderly population. BMC Public Health. 2022;22(1):1382. doi: 10.1186/s12889-022-13759-9.
2. Susilowati R, Rohmanningrum UM. Effective combination of *Nigella sativa* and *Trigonella foenum-graecum* seed extract on wound healing in diabetic mice. Jurnal Biodjati. 2023;8(1):106-16. doi: 10.15575/biodjati.v8i1.19968.
3. Patel S, Srivastava S, Singh MR, Singh D. Mechanistic insight into diabetic wounds: pathogenesis, molecular targets and treatment strategies to pace wound healing. Biomed Pharmacother. 2019;112:108615. doi: 10.1016/j.biopha.2019.108615.
4. Ivanalee AS, Yudaniayanti IS, Yunita MN, Triakoso N, Hamid IS, Saputro AL. Effectiveness of sugar dressing (100% sugar) in improving collagen density in the wound healing process after artificial burn injury in albino rats (*Rattus norvegicus*) skin. J Med Vet. 2018;1(3):134-41.
5. Kmail A, Said O, Saad B. How thymoquinone from *Nigella sativa* accelerates wound healing through multiple mechanisms and targets. Curr Issues Mol Biol. 2023;45(11):9039-59. doi: 10.3390/cimb45110567.
6. Javed A, Usman M, Akram N, Kanwal S, Riaz I, Haider SM. *Nigella sativa* a potent healer for diabetic wounds and its other pharamcognosal attributes. Haya Saudi J Life Sci. 2019;4(4):173-9. doi: 10.21276/haya.2019.4.4.8.
7. Sjakoer N, Mubarakati NJ, Taufiq A. Investigation of excellent ACE inhibitor agents from *Scurrula atropurpure* and *Dendrophthoe pentandra* for anti-hypertension. Chiang Mai Univ J Nat Sci. 2021;20(3):e2021068. doi: 10.12982/cmujns.2021.068.
8. Nusantoro YR, Fadlan A. Analisis sifat mirip obat, prediksi ADMET, dan penambatan molekular isatinil-2-aminobenzoilhidrazon dan kompleks logam transisi Co(II), Ni(II), Cu(II), Zn(II) terhadap BCL2-XL. Akta Kimia Indonesia. 2020;5(2):114-26. doi: 10.12962/j25493736.v5i2.7881.
9. Roy C, Ghosh P. Co-administration of herbal inhibitors of P-glycoprotein with renal drugs enhance their bioavailability–in silico approach. J Herbmed Pharmacol. 2023;12(2):241-9. doi: 10.34172/jhp.2023.26.
10. Fajrin FA, Sulistyowaty MI, Ghiffary ML, Zuhra SA, Panggalih WR, Pratoko DK, et al. Immunomodulatory effect from ethanol extract and ethyl acetate fraction of *Curcuma heyneana* Valeton and Zijp: transient receptor vanilloid protein approach. Heliyon. 2023;9(5):e15582. doi: 10.1016/j.heliyon.2023.e15582.
11. Ugbe FA, Shallangwa GA, Uzairu A, Abdulkadir I. Molecular docking investigation, pharmacokinetic analysis, and molecular dynamic simulation of some benzoxaborole-benzimidazole hybrids: an approach to identifying superior *Onchocerca* inhibitors. Borneo J Pharm. 2023;6(1):58-78. doi: 10.33084/bjop.v6i1.3876.
12. Singh P, Singh VK, Singh AK. Molecular docking analysis of candidate compounds derived from medicinal plants with type 2 diabetes mellitus targets. Bioinformation. 2019;15(3):179-88. doi: 10.6026/97320630015179.
13. Daina A, Michielin O, Zoete V. SwissADME: a free web tool to evaluate pharmacokinetics, drug-likeness and medicinal chemistry friendliness of small molecules. Sci Rep. 2017;7:42717. doi: 10.1038/srep42717.
14. Petrescu AM, Paunescu V, Ilia G. The antiviral activity and cytotoxicity of 15 natural phenolic compounds with previously demonstrated antifungal activity. J Environ Sci Health B. 2019;54(6):498-504. doi: 10.1080/03601234.2019.1574176.
15. Pires DE, Blundell TL, Ascher DB. pkCSM: predicting small-molecule pharmacokinetic and toxicity properties using graph-based signatures. J Med Chem. 2015;58(9):4066-72. doi: 10.1021/acs.jmedchem.5b00104.
16. Bultum LE, Tolossa GB, Kim G, Kwon O, Lee D. In silico activity and ADMET profiling of phytochemicals from Ethiopian indigenous aloes using pharmacophore models. Sci Rep. 2022;12(1):22221. doi: 10.1038/s41598-022-26446-x.
17. Hebert A, Bishop M, Bhattacharyya D, Gleason K, Torosian S. Assessment by Ames test and comet assay of toxicity potential of polymer used to develop field-capable rapid-detection device to analyze environmental samples. Appl Nanosci. 2015;5(6):763-9. doi: 10.1007/s13204-014-0373-7.
18. Asseri AH, Alam MJ, Alzahrani F, Khames A, Pathan MT, Abourehab MA, et al. Toward the identification of natural antiviral drug candidates against Merkel cell polyomavirus: computational drug design approaches. Pharmaceuticals (Basel). 2022;15(5):501. doi: 10.3390/ph15050501.
19. El-Din HM, Loutfy SA, Fathy N, Elberry MH, Mayla AM, Kassem S, et al. Molecular docking-based screening of compounds against VP40 from Ebola virus. Bioinformation. 2016;12(3):192-6. doi: 10.6026/97320630012192.
20. Pratiwi RI, Rahayu T, Mubarakati NJ. In silico screening of *Schleichera oleosa* phytocompounds as estrogen receptors alpha inhibitors for breast cancer. JSMARTech. 2020;2(1):14-21. doi: 10.21776/ub.jsmartech.2020.002.01.14.
21. Nirenjen S, Narayanan J, Tamilanban T, Subramaniyan V, Chitra V, Fuloria NK, et al. Exploring the contribution of pro-inflammatory cytokines to impaired wound healing in diabetes. Front Immunol. 2023;14:1216321. doi: 10.3389/fimmu.2023.1216321.
22. Gelinas AD, Davies DR, Edwards TE, Rohloff JC, Carter JD, Zhang C, et al. Crystal structure of interleukin-6 in complex with a modified nucleic acid ligand. J Biol Chem. 2014;289(12):8720-34. doi: 10.1074/jbc.M113.532697.
23. Zia K, Ashraf S, Jabeen A, Saeed M, Nur-E-Alam M, Ahmed S, et al. Identification of potential TNF-α inhibitors: from in silico to in vitro studies. Sci Rep. 2020;10(1):20974. doi: 10.1038/s41598-020-77750-3.
24. Amrulloh LS, Harmastuti N, Prasetiyo A, Herowati R. Analysis of molecular docking and dynamics simulation of mahogany (*Swietenia macrophylla* King) compounds against the PLpro enzyme SARS-COV-2. J Farm Ilmu Kefarmasian Indones. 2023;10(3):347-59. doi: 10.20473/jfiki.v10i22023.347-359.